

The electronic structure of the silicon vacancy color center in diamond

Christian Hepp,¹ Tina Müller,² Victor Waselowski,³ Jonas N. Becker,¹ Benjamin Pingault,² Hadwig Sternschulte,^{4,5} Doris Steinmüller-Nethl,⁴ Adam Gali,^{6,7} Jeronimo R. Maze,³ Mete Atatüre,² and Christoph Becher^{1,*}

¹*Fachrichtung 7.2 (Experimentalphysik), Universität des Saarlandes, Campus E2.6, 66123 Saarbrücken, Germany*

²*Atomic, Mesoscopic and Optical Physics Group, Cavendish Laboratory,*

University of Cambridge, JJ Thomson Ave, Cambridge CB3 0HE, United Kingdom

³*Departamento de Física, Pontificia Universidad Católica de Chile, Santiago 7820436, Chile*

⁴*KOMET RHOBEST GmbH, 6020 Innsbruck, Austria*

⁵*Fakultät für Physik, Technische Universität München,*

James-Frank-Strasse 1, 85748 Garching, Germany

⁶*Department of Atomic Physics, Budapest University of Technology and Economics, H-1111 Budapest, Hungary*

⁷*Institute for Solid State Physics and Optics, Wigner Research Centre for Physics,*

Hungarian Academy of Sciences, P.O. Box 49, H-1525 Budapest, Hungary

(Dated: October 14, 2013)

The negatively charged silicon vacancy (SiV) color center in diamond has recently proven its suitability for bright and stable single photon emission. However, its electronic structure so far has remained elusive. We here explore the electronic structure by exposing single SiV defects to a magnetic field where the Zeeman effect lifts the degeneracy of magnetic sublevels. The similar response of single centers and a SiV ensemble in a low strain reference sample proves our ability to fabricate almost perfect single SiVs, revealing the true nature of the defect's electronic properties. We model the electronic states using a group-theoretical approach yielding a good agreement with the experimental observations. Furthermore, the model correctly predicts polarization measurements on single SiV centers and explains recently discovered spin selective excitation of SiV defects.

PACS numbers: 81.05.ug, 61.72.jn, 78.55.-m, 71.70.Ej

Negatively charged silicon vacancy (SiV⁻) color centers in diamond show a typical room-temperature zero phonon line (ZPL) at 738 nm which splits into a four line fine structure centered at about 737 nm when cooled down to liquid helium temperature [1–3]. The origin of the fine structure splitting is attributed to a split ground and excited state [1]. One mechanism that can account for the level splitting is spin-orbit (SO) coupling, like it is present for the excited state in negatively charged nitrogen-vacancy (NV⁻) centers [4]. Alternatively, Clark et al. [1] and Moliver [5] suggest a tunnel splitting whereas Goss et al. [6] assume a Jahn-Teller (JT) effect in addition to SO coupling to lift the orbital degeneracy between the electronic states which account for the presumed optical transition ${}^2E_u \rightarrow {}^2E_g$. To form doubly degenerate 2E many-body wave functions, at least a trigonal defect symmetry is required [7, 8]. The molecular structure of the SiV center was predicted using density functional theory (DFT) to show a rather unique split vacancy configuration, exhibiting a D_{3d} symmetry [9]. Yet, polarization [10, 11] and uniaxial stress measurements [2] evidenced lower symmetrical point groups such as C_2 or D_2 symmetry. Still, all these experimental evidences were obtained using samples that possess strongly strained environments for the defect centers. In this letter, however, we present evidence for the predicted D_{3d} symmetry by performing spectroscopy on SiV centers in low-strain samples.

Recently published EPR measurements showed that the presumed neutral charge state SiV⁰ is a $S = 1$ system

[12]. This suggests that its negative counterpart SiV⁻ is a paramagnetic $S = 1/2$ system, although this has not been confirmed by independent EPR measurements so far. Very recently, we reported direct spin-selective population of the SiV⁻ excited states under a magnetic field, resulting in a spin-tagged resonance fluorescence pattern [13], suggesting that the SiV⁻ shows effectively $S = 1/2$. In the present letter, we experimentally explore the electronic states of the SiV center by measuring Zeeman splittings and polarization orientation of the fine structure lines. A detailed theoretical analysis of the SiV⁻ center allows for an assignment of electronic states and correctly describes the Zeeman splittings, polarization properties and earlier measurements on spin-selective excitation [13].

Crucial prerequisites for the experimental investigation of the SiV electronic states are the availability of SiV centers in low strain samples (referred to as “ideal” centers) and the ability to observe isolated single centers in order to prevent inhomogeneous broadening effects. Two samples were investigated: The first (“SiV ensemble sample”) is a thin single crystalline diamond film which contains a large ensemble of SiV defects. The second sample (“SIL sample”) is a high purity bulk diamond in which single SiV centers were created using ion implantation. To enhance the collection of the single emitter fluorescence, an array of solid immersion lenses (SIL) was fabricated using focussed ion beam milling (for details about the samples see Supplemental Material [14]). The samples were investigated in two homebuilt confocal mi-

croscopes, with excitation wavelengths in the range 690 - 700nm, one equipped with a superconducting magnet mounted in Faraday configuration, providing fields up to 7 T. Throughout all measurements, the magnetic field is aligned parallel to the crystallographic [001] direction.

Figure 1 shows the zero-field spectral fine structure of an ensemble of SiV^- defects (Fig. 1(a)) and a single defect under a SIL (SIL1, Fig. 1(c)). The position and splitting (ground state splitting: $\Delta E_g = 50$ GHz (0.21 meV), excited state splitting: $\Delta E_e = 260$ GHz (1.08 meV)) of the fine structure in the SiV^- ensemble sample are in excellent agreement with former findings [1]. The linewidth of the fine structure lines in the SiV^- ensemble is ≈ 10 GHz [3, 13], indicating a very small inhomogeneous broadening and proving the high crystalline quality of the diamond film. Therefore, we treat this SiV^- ensemble as the reference which we compare single SiV^- centers to. For SIL1, the splitting of the two doublets is identical with the reference sample within our resolution limit of 5 GHz. The relative intensity of the peaks is different from the SiV^- ensemble which is due to a different temperature and resulting different thermalization [1].

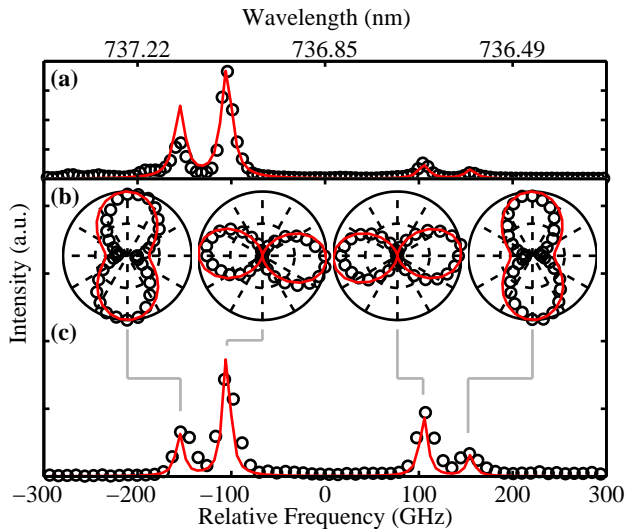


FIG. 1. (Color online) Spectral fine structure of (a) an ensemble of SiV^- centers at 4 K and (c) single emitter SIL1 under a solid immersion lens at 18 K. The inset (b) shows the polarization of each single fine structure line. Black dots: measurements, red solid lines: simulations.

To investigate the dipole transitions of the SiV^- , we measure the photoluminescence polarization for several single emitters in the SIL sample (e.g. SIL1, Fig. 1(b)). The polarization of the fine structure lines can be grouped in two subsets. The inner transitions are polarized parallel to each other and perpendicular to the outer ones, where all polarization axes appear along the $\langle 110 \rangle$ crystal axis. For our measurements, corresponding to a projection into the (001) plane, the observed

polarization direction is consistent with the predicted $\langle 111 \rangle$ orientation of the SiV^- in D_{3d} symmetry [6]. This result is confirmed by independent measurements on a larger number of SiV^- defects [15]. The red solid lines in Fig. 1(c) represent a simulation using the model developed below.

To gain further insight into the electronic structure, both the ensemble of SiV^- and another single emitter, SIL2, were exposed to a magnetic field. The Zeeman effect leads to a splitting of each fine structure line into four lines, where this splitting is not symmetrical and shows several avoided crossings (Fig. 2). The splitting into four components points towards a spin 1/2 system, and the avoided crossings indicate SO coupling. From the fact that the ensemble spectrum shows a very similar splitting pattern to the single defect and splits into as many lines, we learn that all possible equivalent orientations of the center in the ensemble have the same relative angle to the magnetic field. The only orientation which allows for this fact is indeed a $\langle 111 \rangle$ -orientation - which shows for the first time experimental evidence of a $\langle 111 \rangle$ -orientation for SiV^- centers and establishes a link to theories published so far [6, 9].

In the following section, we develop a model of the SiV^- center electronic structure. Starting from the experimental evidence, we model the SiV^- oriented along $\langle 111 \rangle$ direction and assume D_{3d} symmetry [6, 9]. The carbon dangling bond orbitals are superimposed to construct symmetry adapted linear combinations (SALCs) which form the electronic states of the SiV^- center and transform as the irreducible representations A_{1g} , A_{2u} , E_u and E_g . The orbitals belonging to the Si atom can be approximated as hydrogen-like wave functions. DFT calculations yield the ordering of the dangling bond SALCs and Si states, respectively, indicating that the SALCs are considerably lower in energy [16], and that only these need to be considered for optically active transitions [12]. The center hosts a total number of eleven electrons: six electrons contributed by dangling bonds, four electrons from the Si-atom and an electron trapped from nearby donors to account for the negative charge [12]. Taking into account spin degeneracy, the A (E) states accommodate 2 (4) electrons, i.e. one unpaired electron remains in the E_g state. We therefore consider the SiV^- ground state as 2E_g and the excited state as 2E_u where a single hole formalism is equivalent to a single electron state except for signs in spin-orbit interaction [4]. The 2E -states have a twofold orbital and a twofold spin degeneracy. They can be split into (purely spin degenerate) states by either SO or JT interaction. This results in the split ground and excited states with 4 possible optical transitions forming the zero-field ZPL fine structure (Fig. 1). In a magnetic field Zeeman interaction terms $\mathbb{H}_{g,e}^{Z,L}$ and $\mathbb{H}_{g,e}^{Z,S}$ both lift the spin degeneracy ($\mathbb{H}_{g,e}^{Z,L}$ in conjunction with SO coupling). SO, JT and Zeeman interaction sum up to the

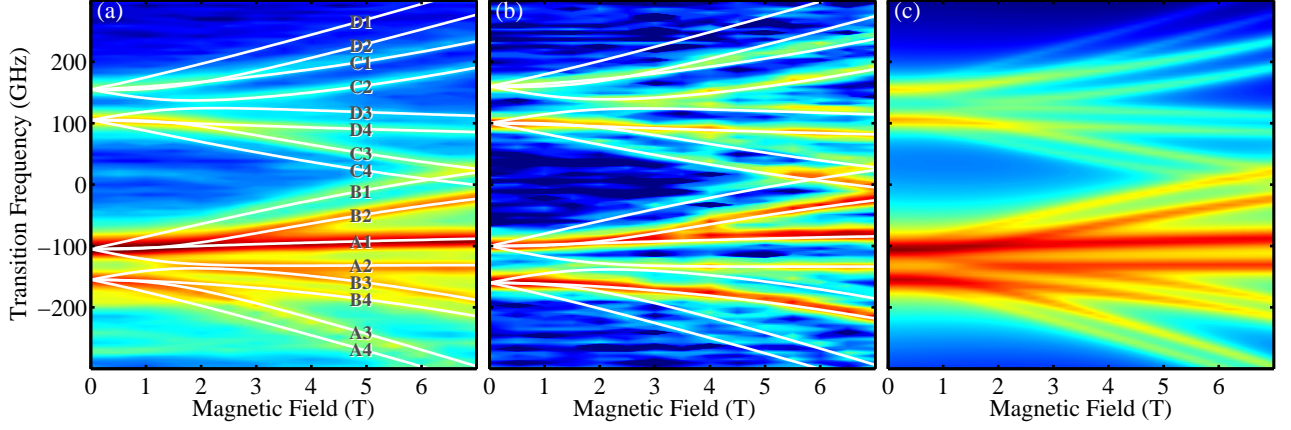


FIG. 2. (Color online) Spectral fine structure splitting of (a) an SiV^- ensemble (contour plot, color coding indicates peak intensity in logarithmic a.u.) and (b) single SiV^- defect under a SIL (SIL2) vs. applied magnetic field (in (001) direction). White solid lines are calculated transitions based on the model mentioned in the text. The labeling of transitions is in accordance with Fig. 3. Panel (c) displays a simulation of the fine structure lines intensity assuming dipolar transitions.

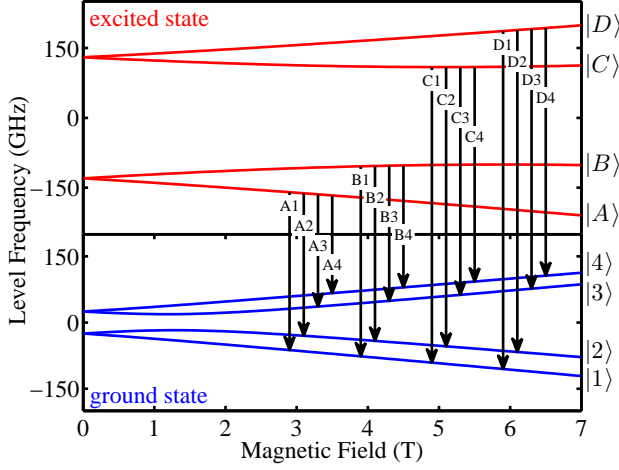


FIG. 3. (Color online) Calculated splitting of electronic levels with increasing magnetic field. Ground and excited state labelled according to the letters and numbers at the right of the panel. Optical transitions between all levels indicated by black arrows and correspond to white solid lines in Fig. 2(a).

following total Hamiltonian for ground or excited state:

$$\begin{aligned} \mathbb{H}_{g,e} &= \mathbb{H}_{g,e}^0 + \mathbb{H}_{g,e}^{\text{SO}} + \mathbb{H}_{g,e}^{\text{JT}} + \mathbb{H}_{g,e}^{\text{Z,L}} + \mathbb{H}_{g,e}^{\text{Z,S}} \\ &= \mathbb{H}_{g,e}^0 + \lambda_{g,e} L_z S_z + \Upsilon_{\text{JT}} + f \gamma_L L_z B_z + \gamma_S \vec{S} \cdot \vec{B}, \end{aligned} \quad (1)$$

where $\mathbb{H}_{g,e}^0$ is the non-perturbed Hamiltonian, $\lambda_{g,e}$ is the SO coupling constant and $\gamma_L = \mu_B/\hbar$, $\gamma_S = 2\mu_B/\hbar$ are orbital and electron gyromagnetic ratios. We express all matrices in the $\{|e_{gx} \uparrow\rangle, |e_{gx} \downarrow\rangle, |e_{gy} \uparrow\rangle, |e_{gy} \downarrow\rangle\}$ basis for the ground state and $\{|e_{ux} \uparrow\rangle, |e_{ux} \downarrow\rangle, |e_{uy} \uparrow\rangle, |e_{uy} \downarrow\rangle\}$ for the excited state: Orbital operators $\langle e|L_r|e\rangle$, $r = x, y, z$, can be directly deduced from the group theoretical description of the NV^- color center in diamond [4]. $\vec{S} = (\sigma_x, \sigma_y, \sigma_z)$

are Pauli spin matrices and Υ_{JT} denotes a $E \otimes e$ linear vibronic JT coupling [17–19], where we define the JT coupling strength $\Upsilon_{g,e} = (\Upsilon_x^2 + \Upsilon_y^2)^{1/2}$ for ground and excited state respectively. We tentatively suggest a factor f which accounts for quenching of the orbital gyromagnetic factor due to JT interaction - a common effect for solid state defect systems [20, 21]. The coordinate frame (internal reference frame) is given by the high symmetry $\langle 111 \rangle$ axis of the SiV which we denote as z axis and x, y in the (111) plane. We have reduced the SO and Zeeman coupling to the expressions in Eq. (1) because under D_{3d} symmetry, L_x and L_y only affect states which transform as A_{1g} and A_{2u} . For each electronic configuration (ground and excited state), the splitting is given by both the SO and JT interactions and is equal to $(\lambda_{g,e}^2 + 4\Upsilon_{g,e}^2)^{1/2}$. This quantity is set equal to the experimentally observed ground and excited state splitting and we use $r_{g,e} = \lambda_{g,e}/\Upsilon_{g,e}$ as free parameters [14].

Solving the secular equation defined by the Hamiltonian in Eq. (1) yields the energies of each state at a given magnetic field value (i.e. the eigenvalues, Fig. 3) as well as their eigenvectors $|1\rangle$ - $|4\rangle$ for ground state and $|A\rangle$ - $|D\rangle$ for excited state, respectively. We calculate the optical transition frequencies between the electronic levels (arrows in Fig. 3, white solid lines in Fig. 2(a)) and compare them with the Zeeman spectrum of our reference sample (Fig. 2(a)). Varying only the quenching factor f and the ratio r_g, r_e between SO and JT in ground and excited state, respectively, we iteratively fit transition frequencies to the experimental data [14]. In both ground and excited state we observe a high SO coupling and only little JT distortion ($r_g = 3.9$, $r_e = 6.2$). As a consequence of the strong SO coupling, Fig. 3 shows a avoided level crossing at 2 T in the ground state which is also a predominant feature in the magnetic field splitting spectra (Fig. 2(a,b)). We note that the fit parameters for the ref-

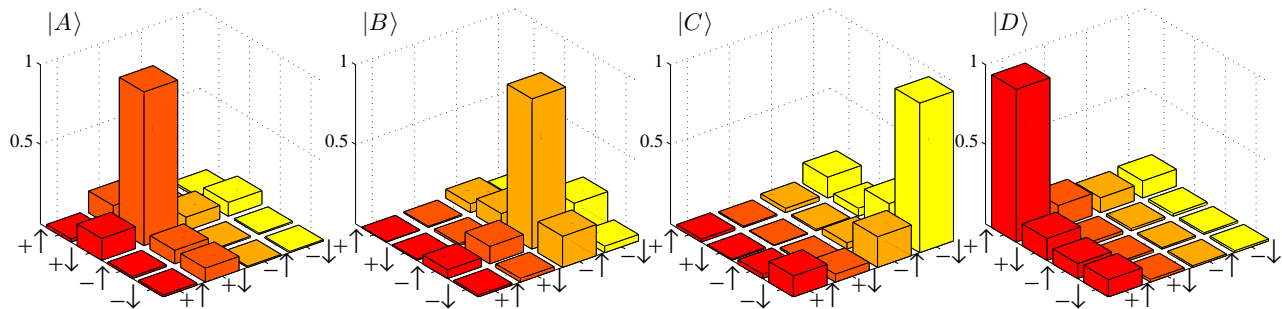


FIG. 4. (Color online) Tomography of the excited states at $B = 4$ T using the model parameters, which lead to the level splitting depicted in Fig. 3. Basis states given in the eigenstates of L_z operator $|e_{\pm}\rangle = -(|e_x\rangle \mp i|e_y\rangle)$ and S_z operator $|\uparrow\rangle, |\downarrow\rangle$.

reference sample (Tab. I) are identical with the parameters for single center SIL2 (within our measurement resolution). This proves our ability to deterministically fabricate “ideal” single SiV centers which reproduce many experimental [1, 2] and theoretical [9] results.

The theoretical model derived here can also be used to assess the applicability of the SiV⁻ center as a quantum bit, i.e. the accessibility of a well defined spin state, as indicated by recent experiments on spin-selective population of SiV⁻ excited states [13]. We are now able to elucidate this phenomenon by calculating the spin and orbital eigenstates of the excited state $|A\rangle$ – $|D\rangle$. Figure 4 displays the absolute value of the excited state density matrix, expressed in basis states of the L_z and S_z operators. As the $[001]$ crystal axis is aligned along the magnetic field direction, the angle between magnetic field and high symmetry axis of the SiV defect is fixed to 54.7° . Therefore, one would expect that Zeeman interaction with off-axis magnetic field terms B_x, B_y leads to spin mixing both in ground and excited state. It is noticeable, however, that in the excited state all electronic states are dominated by contributions from one spin state with a population probability of above 97%, respectively (Fig. 4). The reason for this particular spin polarization is the strong quenching f of the orbital magnetic momentum. In consequence, the spin effectively remains a good quantum number. In contrast, all four ground states show stronger mixing with maximum spin polarization of 80% [14]. We note that the resulting spin orientations in the presence of magnetic field are in full agreement with those reported for spin selective resonant excitation [13]. As the reason for the spin mixing is given by off-axis magnetic field terms, the spin state purity can be further increased by aligning the magnetic field along the SiV high symmetry axis $\langle 111 \rangle$ yielding predicted ground state spin polarizations of above 91% [14].

To further verify the proposed theoretical model, we infer the change in angular momentum for the observed dipole transitions and calculate the expected polarization of the emitted light. The dipole moment $\mathbf{d} = \langle f|\mathbf{r}|i\rangle$, with $|i\rangle = |A\rangle \dots |D\rangle$ and $\langle f| = \langle 1| \dots \langle 4|$, is directly de-

TABLE I. Fit parameters for SiV reference ensemble (“ensemble” sample) and single defects depicted above.

Emitter name	f	λ_g	$\Upsilon_{x,g}$	$\Upsilon_{y,g}$	λ_e	$\Upsilon_{x,e}$	$\Upsilon_{y,e}$	ΔE_g	ΔE_e
	(-)				(GHz)				
Ensemble	0.1	45	11	257	20	50	260		
SIL1 (Fig. 1(c))	0.1	49	2	3	257	12	16	50	260
SIL2 (Fig. 2(b))	0.1	54	14	257	20	60	260		

rived from the numerically determined eigenvectors. We then project the emitted linear and circular polarization components onto our observation plane (001) and use the numerical method of Ref. [22] to estimate the relative collection efficiencies of our experimental setup for different dipole components. The result includes both the polarization direction and visibility (red line in Fig. 1). Starting from parameters of an ideal SiV⁻ (Tab. I, “ensemble”), we fit the fluorescence polarization of emitter SIL1 (Fig. 1(c)) and obtain comparable parameters (Tab. I, “SIL1”). We note, that the polarization of the first and second peak is tilted by $8 \pm 4^\circ$ away from $\langle 110 \rangle$ direction. We model this polarization change by adjusting JT distortion parameters Υ_x and Υ_y ; a similar result would be obtained using a static strain addition. The calculation of the dipole transition strength further allows the reconstruction of the Zeeman spectrum at arbitrary magnetic field values (Fig. 2(c)) yielding an impressive agreement with the measured data (Fig. 2(a)).

We note that the spectra and polarization graphs of Fig. 1(a-c) correspond to the case of ideal, strain-free SiV centers. Different Zeeman splitting patterns as well as polarization directions and visibilities have been experimentally observed in other regions of the SIL sample and in nanodiamonds. These deviations can be explained by the influence of crystal strain in the host lattice. The addition of a phenomenological strain Hamiltonian to the theoretical model faithfully reproduces these variations (to be published elsewhere). The variation of polarization direction under strain further might explain the lower de-

fect symmetry inferred from SiV⁻ polarization data in strained diamond samples [2, 10, 11].

In conclusion, we demonstrated the fabrication of unstrained, single SiV⁻ centers that allow for the study of the center's unperturbed electronic structure. Our theoretical model explains both the SiV⁻ fine structure splitting in magnetic fields as well as the polarization of the zero field fine structure components. Furthermore, it provides a qualitative explanation of the first spin-related experiments of the negatively charged SiV. This profound understanding paves the way for utilizing the SiV⁻ center in quantum information applications.

We thank David Steinmetz and Jan Meijer for ion implantation of the SILs sample and Elke Neu for helpful discussions. Ion implantation was performed at and supported by RUBION, central unit of the Ruhr-Universität Bochum. We are deeply grateful to Christoph Pauly and Frank Mücklich from the Functional Materials Group at the Saarland University for SIL fabrication and Annika S. Diehl for automizing polarization measurements. C.B. acknowledges funding from the Bundesministerium für Bildung und Forschung within the projects EPHQUAM (Contract No. 01BL0903) and QuORep (Contract No. 01BQ1011). M.A. gratefully acknowledges financial support by the University of Cambridge, the European Research Council (FP7/2007-2013)/ERC Grant agreement no. 209636 and FP7 Marie Curie Initial Training Network S³NANO. A.G. acknowledges the support from EU Commission by the FP7 DIAMANT project (No. 270197). V.W. thanks CONICYT-PCHA/Doctorado Nacional/2013-21130747 for financial support. J.R.M. acknowledges support from Concicyt Fondecyt Iniciacin no. 11100265 and PIA no. ACT1108..

* christoph.becher@physik.uni-saarland.de

- [1] C. D. Clark, H. Kanda, I. Kiflawi, and G. Sittas, Phys. Rev. B **51**, 16681 (1995).
 [2] H. Sternschulte, K. Thonke, J. Gerster, W. Lim-

- mer, R. Sauer, J. Spitzer, and P. C. Münzinger, Diam. Relat. Mater. **4**, 1189 (1995).
 [3] E. Neu, C. Hepp, M. Hauschild, S. Gsell, M. Fischer, H. Sternschulte, D. Steinmüller-Nethl, M. Schreck, and C. Becher, New J. Phys. **15**, 043005 (2013).
 [4] J. R. Maze, A. Gali, E. Togan, Y. Chu, A. Trifonov, E. Kaxiras, and M. D. Lukin, New J. Phys. **13**, 025025 (2011).
 [5] S. S. Moliver, Tech. Phys. **48**, 1449 (2003).
 [6] J.P. Goss, R. Jones, S.J. Breuer, P.R. Briddon, and S. Öberg, Phys. Rev. Lett. **77**, 3041 (1996).
 [7] M. Tinkham, *Group theory and quantum mechanics* (Dover Publications, Mineola, N.Y., 1964).
 [8] J. Walker, Reports Prog. Phys. **42**, 1605 (1979).
 [9] J. P. Goss, P. R. Briddon, and M. J. Shaw, Phys. Rev. B **76**, 075204 (2007).
 [10] S. Brown and S. Rand, J. Appl. Phys. **78**, 4069 (1995).
 [11] E. Neu, M. Fischer, S. Gsell, M. Schreck, and C. Becher, Phys. Rev. B **84**, 205211 (2011).
 [12] U. F. S. D'Haenens-Johansson, A. M. Edmonds, B. L. Green, M. E. Newton, G. Davies, P. M. Martineau, R. U. A. Khan, and D. J. Twitchen, Phys. Rev. B **84**, 245208 (2011).
 [13] T. Müller, C. Hepp, B. Pingault, E. Neu, S. Gsell, M. Schreck, H. Sternschulte, D. Steinmüller-Nethl, C. Becher, and M. Atatüre, submitted.
 [14] "See Supplemental Material at [URL will be inserted by publisher] for details on samples, experimental setup, theoretical model, polarization curve simulation and spin state tomography."
 [15] L. J. Rogers, K. D. Jahnke, M. W. Doherty, A. Dietrich, L. Mcguinness, M. Christoph, T. Teraji, J. Isoya, N. B. Manson, and F. Jelezko, in preparation.
 [16] A. Gali and J. R. Maze, arXiv:1310.2137v1.
 [17] T. A. Abtew, Y. Y. Sun, B.-C. Shih, P. Dev, S. B. Zhang, and P. Zhang, Phys. Rev. Lett. **107**, 146403 (2011).
 [18] J. Rorison and M. O'Brien, J. Phys. C Solid State Phys. **17**, 3449 (1984).
 [19] H. C. Longuet-Higgins, U. Opik, M. H. L. Pryce, and R. A. Sack, Proc. R. Soc. A Math. Phys. Eng. Sci. **244**, 1 (1958).
 [20] F. S. Ham, Phys. Rev. **138**, 1727 (1965).
 [21] E. Tosatti, N. Manini, and O. Gunnarsson, Phys. Rev. B **54**, 17184 (1996).
 [22] E. Neu, M. Agio, and C. Becher, Opt. Express **20**, 19956 (2012).